

 <p>ISSN NO. 2320-5407</p>	<p>Journal Homepage: - www.journalijar.com</p> <p>INTERNATIONAL JOURNAL OF ADVANCED RESEARCH (IJAR)</p> <p>Article DOI: 10.21474/IJAR01/21491 DOI URL: http://dx.doi.org/10.21474/IJAR01/21491</p>	 <p>INTERNATIONAL JOURNAL OF ADVANCED RESEARCH (IJAR) ISSN 2320-5407 Journal Homepage: http://www.journalijar.com Journal DOI: 10.21474/IJAR01</p>
---	--	--

RESEARCH ARTICLE

NUMERICAL RESOLUTION OF THE NON-LINEAR NON-ISOTROPIC DIFFUSION EQUATION IN DIMENSION 2 WITH NOISE EFFECT: APPLICATION TO IMAGE PROCESSING.

Atidecou Didier L. NOUMON¹, V. M. Serge SOUMANOU¹, Adébayo Louis ESSOUN¹, Siaka MASSOU¹

¹. Laboratory of Theoretical Physics and Mathematical Physics. University of Abomey-Calavi (Benin)

Manuscript Info

Manuscript History

Received: 05 June 2025

Final Accepted: 07 July 2025

Published: August 2025

Key words:-

Numerical resolution ; non-isotropic non linear diffusion equation ; noise.

Abstract

The application of the numerical resolution of partial differential equations to images constitutes one of the types of tools used in image processing. From the work thus carried out, it emerges, following the analysis of the objective statistical criteria obtained, that the proposed model, in particular that with the effect of colored noise, enables more effective filtering of images compared with the Perona-Malik model and with the Catte et Al model for certain well-defined values of the study parameters.

"© 2025 by the Author(s). Published by IJAR under CC BY 4.0. Unrestricted use allowed with credit to the author."

Introduction:-

The importance of using images in all areas of our contemporary societies is no longer in doubt. Images have an important place in meteorology; in astronomy; in medicine, etc. The different sensors and devices used (satellites; cameras; telescopes, etc.) in the process of acquiring and processing images inevitably insert noise that alters the quality of these images. Thus, the design of image processing tools is essential. One of these tools is the use of partial differential equations for various operations such as contour detection, restoration [1, 9], registration, image segmentation [2, 9].

The heat model is one of the first mathematical models used in image processing to perform linear filtering. The heat equation model, when used in image processing, does not distinguish between image edges and noise. It eliminates noise and significantly degrades image edges. This affects image quality. To then address the problem of non-detection of edges, modifications were made to the heat equation model through several works. Thus, [4] introduced an important improvement to the theory of edge detection. They propose to replace the equation of heat by a nonlinear equation.

$$\begin{cases} \frac{\partial u}{\partial t} = \text{div}(g(\|\nabla u\|)\nabla u) & \text{in }]0; T[\times \Omega \\ \frac{\partial u}{\partial N} = 0 & \text{on }]0; T[\times \partial\Omega \\ u(X, 0) = u_0(X), & \forall X \in \Omega \end{cases} \quad (1.1)$$

Where div and ∇ indicate the divergent and gradient operators with respect to the spatial variables respectively and g is a decreasing function $\mathbb{R}^+ \rightarrow \mathbb{R}^+$, we can choose for example:

$$g(\|\nabla u\|) = \exp\left(-\frac{(\|\nabla u\|)^2}{\delta^2}\right) \quad (1.2)$$

Corresponding Author:- Atidecou Didier L. NOUMON.

Address: Laboratory of Theoretical Physics and Mathematical Physics. University of Abomey-Calavi

Or else
$$g(\|\nabla u\|) = \frac{1}{1 + \frac{\|\nabla u\|^2}{\delta^2}} \quad (1.3)$$

If $g = 1$, we find the heat equation. We often impose $\lim_{t \rightarrow \infty} g(t) = 0$ and $g(0) = 1$.

g is the diffusivity function plays a critical role in performing nonlinear diffusion filtering. And δ is the parameter called "diffusion threshold or barrier".

This model has several drawbacks, the first of which is its ineffectiveness in areas where the noise has large discontinuities. The second drawback is theoretical for the previous g functions because it has been shown that there is no solution to the equation (1.1). Indeed, $\|\nabla u\| \cdot g(\|\nabla u\|)$ is decreasing.

The Catte et al model corrects the ill-posed problem of the Perona-Malik model by introducing a regularization [5]. Thus the new equation (1.4) admits a solution whose existence and uniqueness have been proven [7].

The difference between the Perona-Malik model and that of Catte et al is that in the latter model, the gradient of the image ∇u in the diffusivity function $g(\|\nabla u\|)$, is replaced by $\nabla G_\sigma * u$ where $G_\sigma = C \cdot \sigma^{\frac{1}{2}} \cdot \exp\left(-\frac{x^2}{4\sigma}\right)$ (fundamental solution of the heat equation [7]).

$$\begin{cases} \frac{\partial u}{\partial t} = \text{div}(g(\|\nabla G_\sigma * u\|)\nabla u) & \text{in }]0; T[\times \Omega \\ \frac{\partial u}{\partial N} = 0 & \text{on }]0; T[\times \partial\Omega \\ u(X, 0) = u_0(X), & \forall X \in \Omega \end{cases} \quad (1.4)$$

Where $u_0(x, y)$ constitutes the initial image to be processed $u(x, y, t)$ is the smoothed image at the scale referenced by the parameter t and $g(\|\nabla u\|)$ is a decreasing function of the variable $\|\nabla u\|$ which tends towards 0 when $\|\nabla u\|$ tends towards infinity.

The discretized form of the equation (1.4) which takes the following form [7]:

$$u_{i,j}^n = \left[1 + \frac{\Delta t}{2h^2} (4\alpha_{i,j}^n + \alpha_{i-1,j}^n + \alpha_{i+1,j}^n + \alpha_{i,j-1}^n + \alpha_{i,j+1}^n) \right] u_{i,j}^{n+1} - \frac{\Delta t}{2h^2} (\alpha_{i-1,j}^n + \alpha_{i,j}^n) u_{i-1,j}^{n+1} - \frac{\Delta t}{2h^2} (\alpha_{i,j}^n + \alpha_{i+1,j}^n) u_{i+1,j}^{n+1} - \frac{\Delta t}{2h^2} (\alpha_{i,j-1}^n + \alpha_{i,j}^n) u_{i,j-1}^{n+1} - \frac{\Delta t}{2h^2} (\alpha_{i,j}^n + \alpha_{i,j+1}^n) u_{i,j+1}^{n+1} + f(u_{i,j}^{n+1}) \quad (1.5)$$

The advantages of the Catté et al model over the Perona-Malik model are as follows: the Catté et al model, unlike that of Perona-Malik, in the case of a noisy image, makes the distinction between noise and edges. Thus the latter are preserved even for a noisy image. Indeed, the diffusivity function $g(\|\nabla G_\sigma * u\|)$ only diffuses if the image gradient is weak; moreover the term $\|G_\sigma\|$ removes noise [7]. This partial differential equation is a well-posed problem unlike the Perona-Malik model [7].

Apart from the models described above, many other mathematical models are used in image processing. We can cite that of Morfu [8] which is based on the numerical resolution of the anisotropic nonlinear diffusion equation (1.6).

$$\frac{\partial u}{\partial t} = \text{div}(g(\|\nabla u\|)\nabla u) + f(u) \quad (1.6)$$

where $f(X)$ a non-linearity which is most often expressed in the following cubic form:

$$f(X) = -\beta X(X - \alpha)(X - 1) \quad (1.7)$$

The explicit discretization numerical scheme was used. The results obtained show that this model allows for noise filtering and contrast enhancement of images while preserving the image contours. One of the disadvantages of this model is its sensitivity to noise. When the noise increases slightly, the results obtained are unsatisfactory.

The objective of our work in this article is to : modify the model (1.4) proposed by [5] by introducing the effects of white and colored noise ; numerically solving this new model ; finally applying the numerical resolution to the noisy images in order to process them. Thus in the second section we proceed to the numerical resolution of the anisotropic nonlinear diffusion equation with the effects of white and colored noise; then we applied the resolution of the equation to the noisy images through the third section. We evaluated the quality of the processed images in the fourth section. Finally, in the fifth section, we concluded.

2- Numerical resolution of the proposed model

2.1- Numerical diagram of the proposed model

The numerical method used to solve the equation (1.7) is the finite difference method. Referring to the model of Catté et al [8] and adding the term $f(u)$, we obtain the implicit numerical scheme obtained is the following :

$$u_{i,j}^{n+1} = \left[1 + \frac{\Delta t}{2h^2} (4\alpha_{i,j}^n + \alpha_{i-1,j}^n + \alpha_{i+1,j}^n + \alpha_{i,j-1}^n + \alpha_{i,j+1}^n) \right] u_{i,j}^{n+1} - \frac{\Delta t}{2h^2} (\alpha_{i-1,j}^n + \alpha_{i,j}^n) u_{i-1,j}^{n+1} - \frac{\Delta t}{2h^2} (\alpha_{i,j}^n + \alpha_{i+1,j}^n) u_{i+1,j}^{n+1} - \frac{\Delta t}{2h^2} (\alpha_{i,j-1}^n + \alpha_{i,j}^n) u_{i,j-1}^{n+1} - \frac{\Delta t}{2h^2} (\alpha_{i,j}^n + \alpha_{i,j+1}^n) u_{i,j+1}^{n+1} + f(u_{i,j}^{n+1}) \quad (2.1)$$

The initial condition is expressed as follows:

$$u_{i,j}^0 = u_0(ih, jh) \quad 0 \leq i \leq N+1, \quad 0 \leq j \leq N+1$$

The boundary conditions are expressed by the following relations:

$$u_{i,0}^{n+1} = u_{i,1}^{n+1} \quad u_{N,j}^{n+1} = u_{N+1,j}^{n+1} \quad 0 \leq i \leq N+1, \quad 0 \leq j \leq N+1 \quad (2.3)$$

$$u_{0,j}^{n+1} = u_{1,j}^{n+1} \quad u_{i,N}^{n+1} = u_{i,N+1}^{n+1} \quad 0 \leq i \leq N+1, \quad 0 \leq j \leq N+1 \quad (2.4)$$

The discrete problem (2.1) can be written in the following matrix form:

$$u^n = (I + \Delta t \cdot A_h(u^n)) u^{n+1} + f(u^{n+1}), \quad n \geq 0 \quad (2.5)$$

The white noise and colored correlation functions are given the equations (2.6) and (2.7) [10].

$$f(x) = 2D\delta(x) \quad (2.6)$$

$$f(x) = \frac{D}{\tau} \exp\left(-\frac{|x|}{\tau}\right) \quad (2.7)$$

D : Diffusion coefficient.

τ : Relaxation time.

The Matrix A_h is block tridiagonal and positive definite. By classical arguments [7], the matrix $I + \Delta t \cdot A_h(u^n)$ is invertible.

Solving the matrix equation (2.5) will be applied to process images.

The numerical solution of the differential equation for different values of the parameters λ ; Δt ; $\Delta x = 1$; $\Delta y = 1$, is presented by the figures below for white noise on the one hand and colored noise on the other hand.

2.2- Evaluation of the quality of denoised images

The relevance of noise reduction methods depends on two criteria for evaluating their effectiveness.

We have the subjective criterion and the objective criteria.

The subjective criterion represents the visual aspect, it allows to identify the content of the images, their sharpness, the presence of artifacts and the quality of the contours [18].

The objective criterion is based on three measures: the mean square error (MSE); the signal-to-noise ratio (PSNR) and the structural similarity index (SSIM). Although they do not always correspond with human perception, they allow us to measure the fidelity of an image evaluation.

Mean Squared Error (MSE):

$$MSE = \sum_{i=1}^M \sum_{j=1}^N (X(i,j) - \tilde{X}(i,j))^2$$

X : Original image.

\tilde{X} : denoised image.

M : Number of lines on the image.

N : Number of columns on the image.

(i, j) : Pixel positioning.

Peak Signal to Noise Ratio (PSNR):

$$PSNR = 10 \log_{10} \left(\frac{255^2}{MSE} \right)$$

where 255 is the maximum value of a pixel for an image encoded by 8 bits/pixel in grayscale.

Structural Similarity Index Measure:

It allows you to measure the similarity between two images.

$$SSIM = \frac{(2\mu_x \cdot \mu_y + C_1)(\sigma_{xy} + C_2)}{(\mu_x^2 + \mu_y^2 + C_1)(\sigma_x^2 + \sigma_y^2 + C_2)}$$

μ_x : mean of the pixel sample of x;

μ_y : mean of the pixel sample of y;

σ_x^2 : variance of x;

σ_y^2 : variance of y;

σ_{xy} : covariance of x and y;

$C_1 = (k_1 \cdot L)^2$; $C_2 = (k_2 \cdot L)^2$; $k_1 = 0,01$; $k_2 = 0,03$.

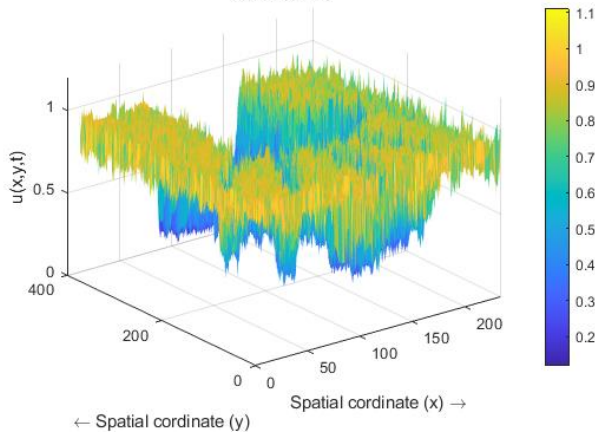
To evaluate the performance of our model, we compare it with the models of Perona-Malick and Catté et al according to the criteria defined above.

- The smaller the mean square error (MSE), the better the model performs.
- The higher the peak signal-to-noise ratio (PSNR), the better the model performs.
- The closer the structural similarity index (SSIM) is to 1, the better the model performs.

2.3 -Numerical solution of the anisotropic nonlinear diffusion equation

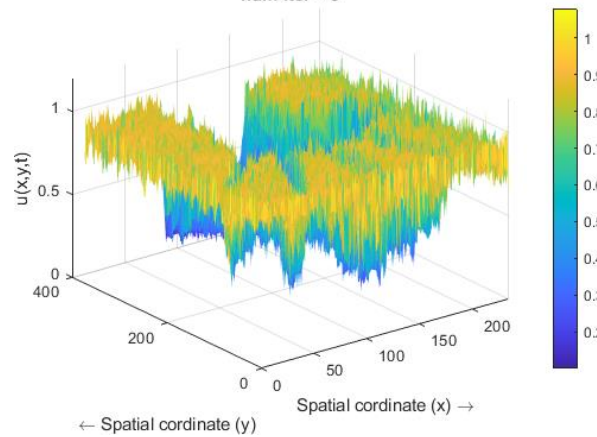
The diffusivity function used is that given by the relation (1.3).

Non-linear non-isotropic diffusion equation with effect of colored noise
delta-t=0.01
num-iter = 8

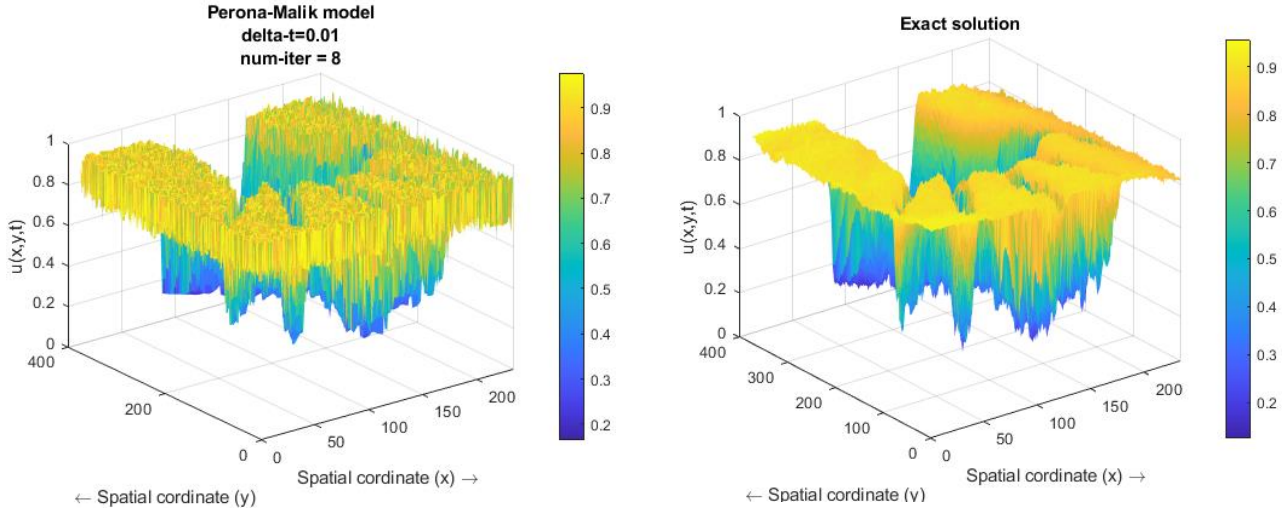


(a) Solution with colored noise effect

Catté and Al model
delta-t=0.01
num-iter = 8



(b) Solution with the Catté et Al model



(c) Solution with the Pérona-Malik model

(d) exact solution

Figure 1 – Numerical solution of the nonlinear nonisotropic equation in dimension 2

3. Numerical results and analyses

The simulations were carried out under Matlab with the following parameters $\Delta t = \frac{1}{100}$; $\Delta x = 1$; $\Delta y = 1$; the initial value of u is the noisy grayscale image; four (4) iterations were made for the first simulation. The number N of mesh points in each of these directions corresponds to the dimensions of the image.

The diffusion threshold λ that we propose is determined by the relation (3.1).

$$\lambda = \frac{\sqrt{K_1^2 + K_2^2 + K_3^2}}{3} \quad (3.1)$$

K_1 is the diffusion threshold proposed by Black et al [16]. It is determined by the relation (3.2).

$$K_1 = \frac{1,4826}{\sqrt{2}MAD(\Delta u)} \quad (3.2)$$

$$MAD(\Delta u) = \text{mediane}(\|\Delta u\| - \text{mediane}(\|\Delta u\|))$$

K_2 is the diffusion threshold proposed by Black et al [17]. It is determined by the relation (3.3).

$$K_2 = \beta \cdot \sqrt{\text{mean}(\|\Delta u\|^2)} \quad (3.3)$$

$$\beta \in [0,6 ; 1,2]$$

K_3 is the diffusion threshold proposed by Morfu [8] of which $K_3 = 0.03783$.

3.1- Application of the numerical solution of the nonlinear anisotropic scattering equation to greyscale images:

The model (2.5) designed is used to denoise the noisy image (image b) from which the original image (image a) is known. The approach is thus proposed in order to ultimately compare the denoised image with the original image in order to make an objective and accurate assessment of the proposed model.

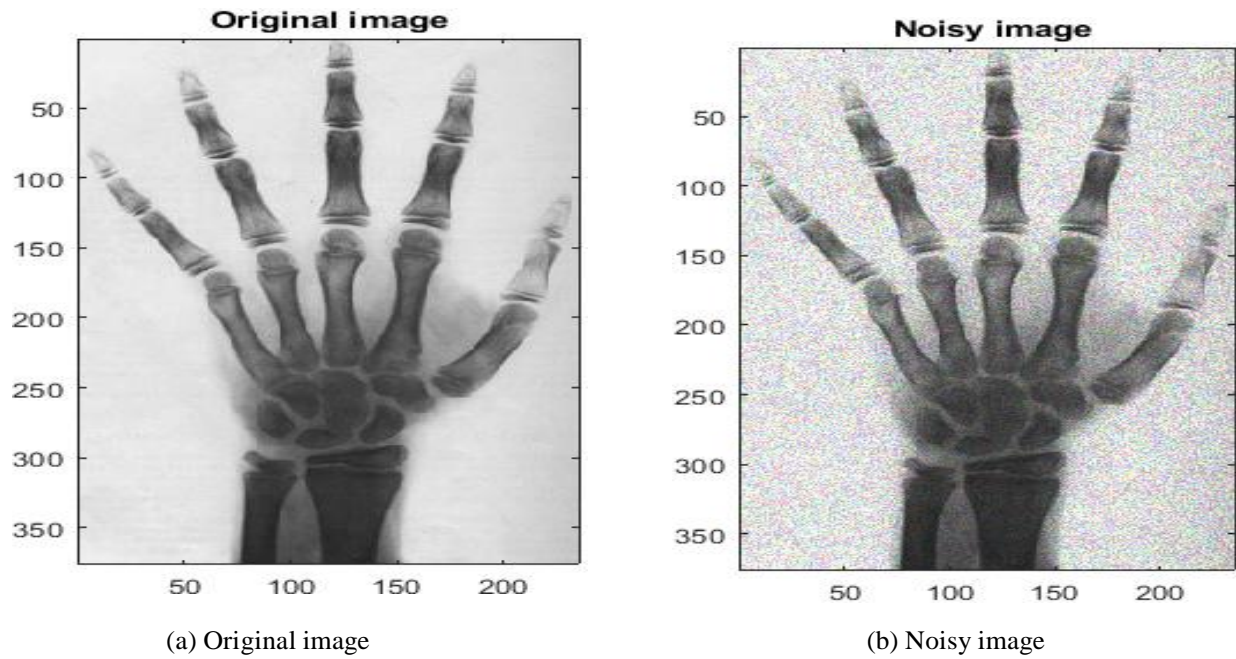
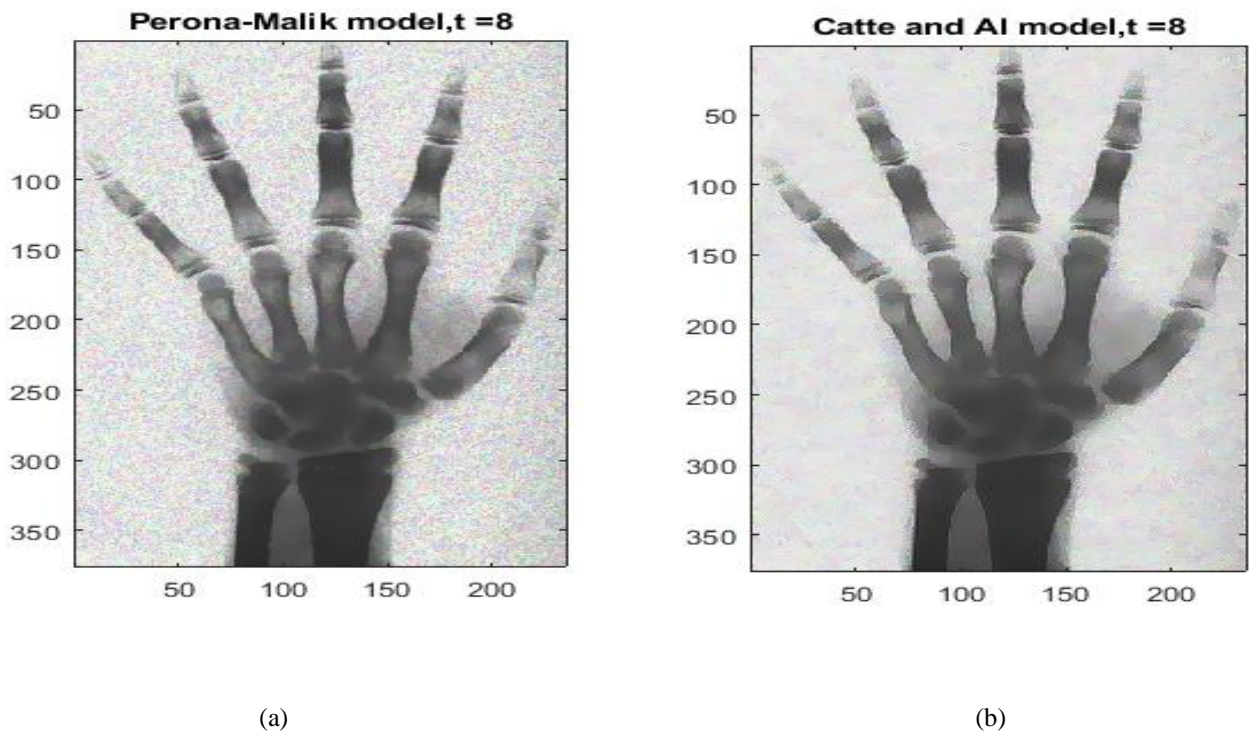


Figure 2 – Original image and noisy image.



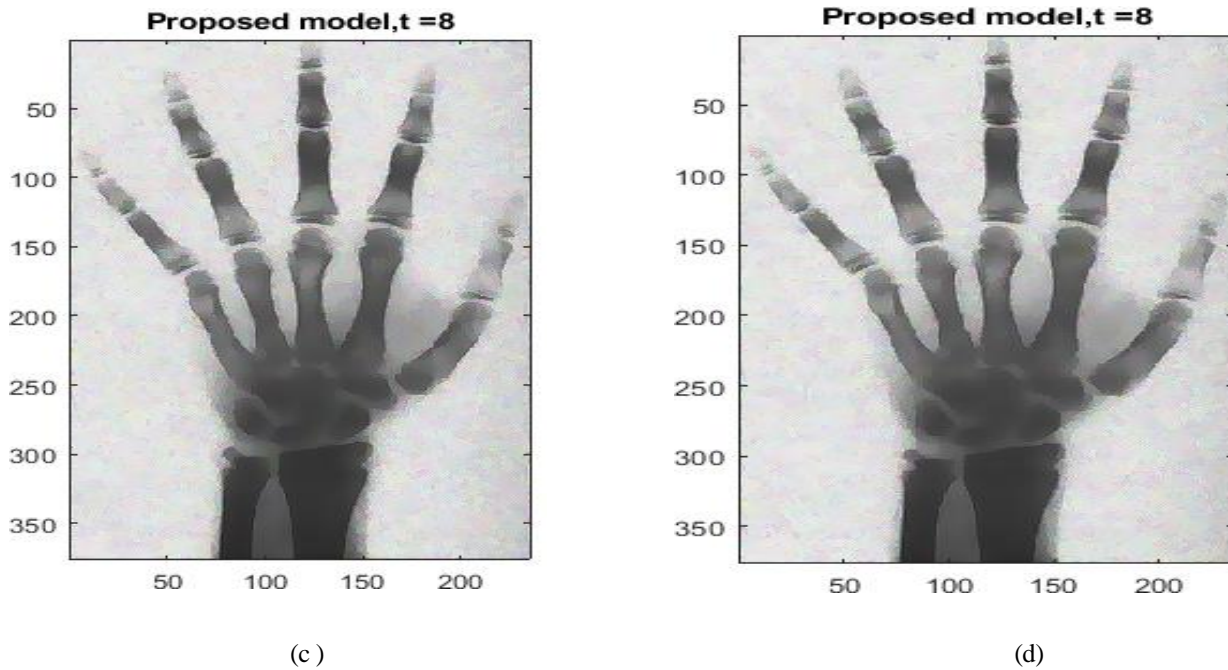


Figure 3: Comparison of the proposed model with white and colored noise effect with the Catte and Perona-Malik models. (a) Perona-Malik model; (b) Catte and AI model; (c) Proposed model with white noise effect; (d) Proposed model with colored noise effect.

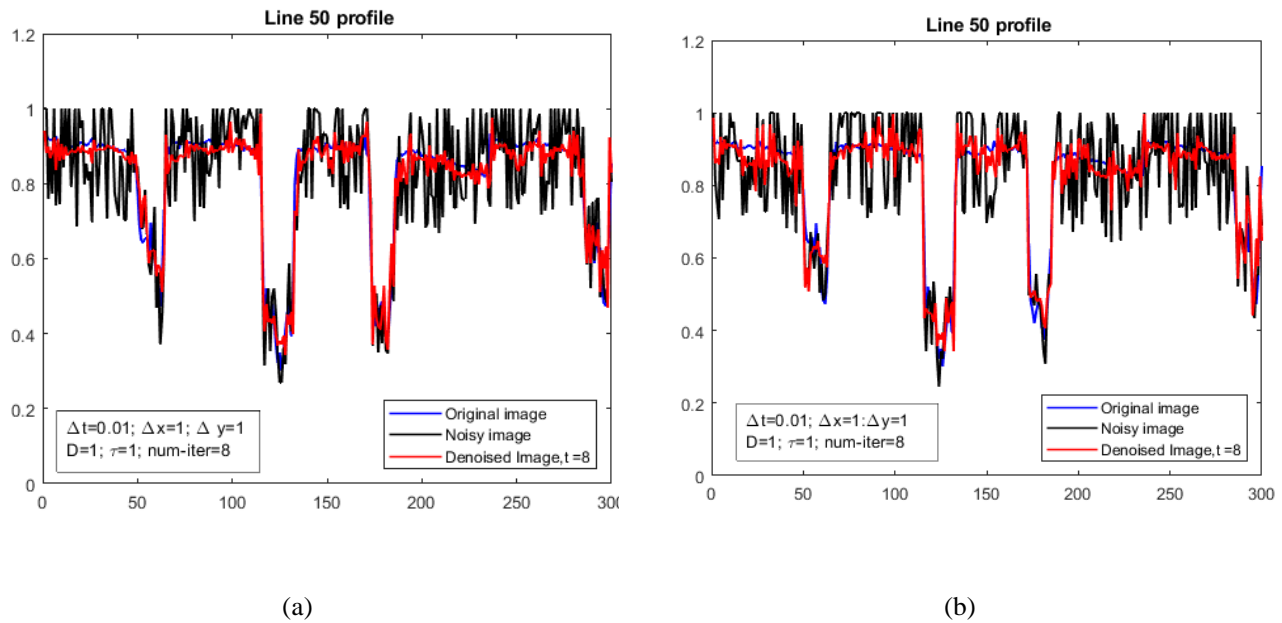


Figure 4: Comparison of line 50 profiles of images restored by the proposed model with white and colored noise effects. (a) Comparison of line 50 profile of images restored by the proposed model with white noise effects. (b) Comparison of line 50 profile of images restored by the proposed model with colored noise effects.

The shape of the profile of line 50 of the image denoised by the proposed model with white noise effect is close to that of the profile of line 50 of the original image. The proximity of the two curves is even greater in the case of the model with colored noise effect. This means that the model enables efficient denoising of an image with the white noise effect as well as the colored noise effect. However, it's important to point out that the denoising performed by the model with the colored noise effect is better than the denoising with the white noise effect.

3.2-Assessing restored images using objective criteria

In order to provide a relevant analysis and interpretation of the mean square deviation (MSE), the peak signal-to-noise ratio (PSNR) and the structural similarity index (SSIM), these criteria are proposed in the form of curves

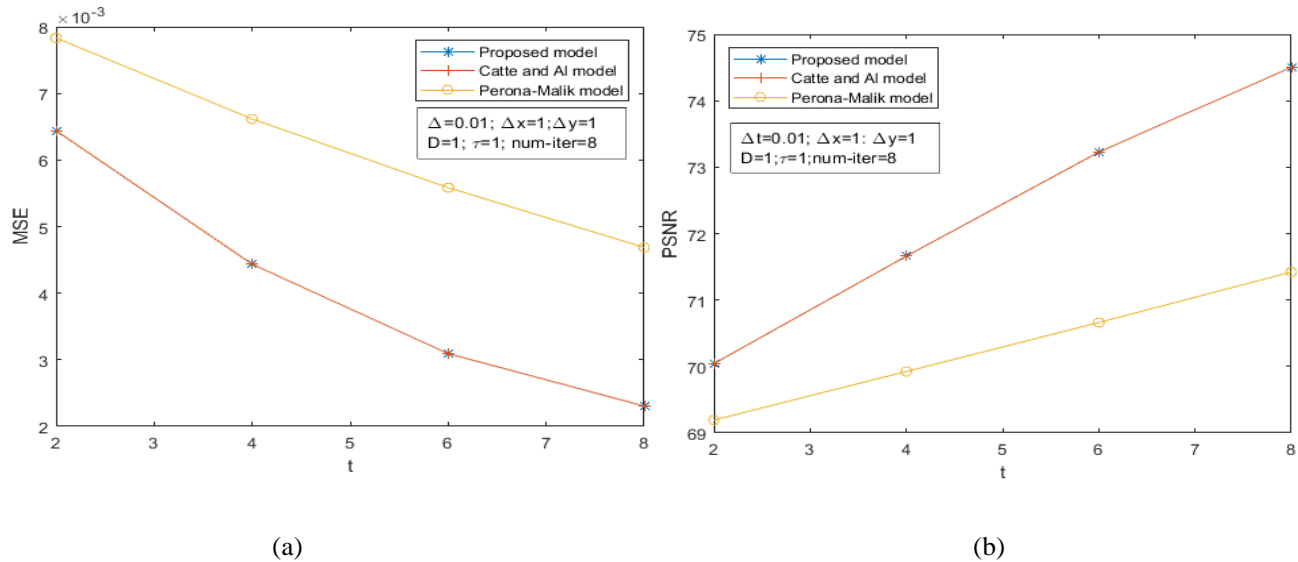


Figure 5: Mean square deviation (MSE) and peak signal-to-noise ratio (PSNR) of the proposed model with white noise effects. (a) Comparison of the mean square deviations of the proposed model with white noise effects. (b) Comparison of the peak signal-to-noise ratio (PSNR) of the proposed model with white noise effects

Curves (a) and (b) in Figure 5 show, respectively, the variations in the mean square deviation (MSE) and the peak signal-to-noise ratio (PSNR) of the proposed model with the effect of white noise, those of Catte and Perona-Malik. These curves indicate that as the control parameter (t) increases, the mean square deviation (MSE) decreases while the peak signal-to-noise ratio (PSNR) increases. These respective variations in these two objective criteria for assessing the models show an improvement in the quality of the image denoised by each of these models. However, it is important to point out that the mean square deviation of the proposed model with the white noise effect is almost identical to that of the Catte et Al model, but is below the curve of the Perona-Malik model. The proposed model with the white noise effect, like the Catte et Al model, therefore provides better denoising of the noisy image than the Perona-Malik model.

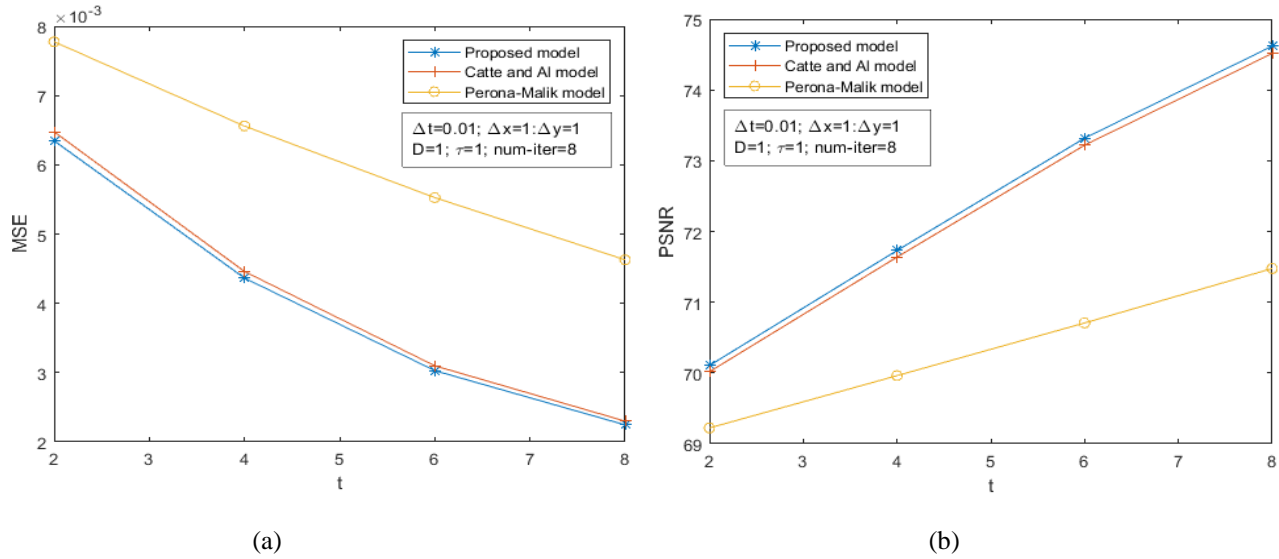


Figure 6: Mean square deviation (MSE) and peak signal-to-noise ratio (PSNR) of the proposed model with colored noise effects. (a) Comparison of the mean square deviations of the proposed model with colored noise effects. (b) Comparison of the peak signal-to-noise ratio (PSNR) of the proposed model with colored noise effects.

As in the previous case, the curves (a) and (b) in Figure 6, showing respectively the variations in the mean square deviation (MSE) and the peak signal-to-noise ratio (PSNR) of the proposed model with the effect of colored noise, those of Catte and Perona-Malik, decrease and increase respectively. These respective variations in mean square deviation (MSE) and peak signal-to-noise ratio (PSNR) indicate an improvement in the quality of the image denoised by each of these models. Nevertheless, it should be noted that the curve (a) indicating the variations in the mean square deviation (MSE) of the proposed model with the colored noise effect is clearly below the curves for the Catte et Al and Perona-Malik models, and the curve (b) indicating the variations in the peak signal-to-noise ratio (PSNR) is clearly above the Catte et Al and Perona-Malik models. Thus the proposed model with the colored noise effect provides better image denoising than the Catte et Al and Perona-Malik models.

In the end, the model proposed with the colored noise effect achieves better denoising than the model proposed with the white noise effect.

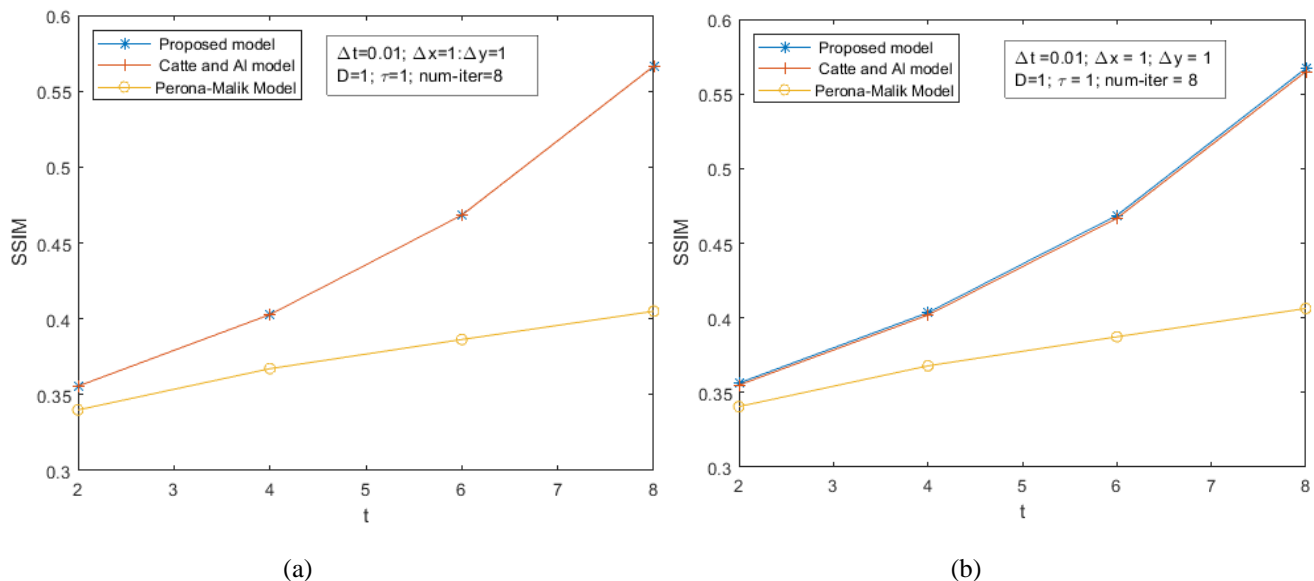


Figure 7 – Comparison of the structural similarity indices (SSIM) of the proposed model with white noise and colored noise effects. (a) Comparison of the structural similarity indices (SSIM) of the proposed model with white noise effects. (b) Comparison of the structural similarity indices (SSIM) of the proposed model with colored noise effects.

The curve (a) in Figure 7, showing the variations in the structural similarity index (SSIM) of the proposed model with the white noise effect is almost identical to that of the Catte et Al model, but is above the curve for the Perona-Malik model. The proposed model with white noise effect, like the Catte et Al model, therefore achieves better denoising of the noisy image than the Perona-Malik model.

For the proposed model with the effect of colored noise, curve (b) showing the variations in the structural similarity index (SSIM) of the proposed model with the effect of colored noise is above the curves for the Catte et Al and Perona-Malik models.

A comparative study of the curves in Figure 7 shows that the proposed model provides better restoration of the noisy image than the Catte et Al and Perona-Malik models. In addition, it is important to point out that the proposed model with the colored noise effect achieves better denoising than the proposed model with the white noise effect.

Conclusion:-

In our work, we began with a brief review of the state of the art of noise in image processing. As an application, the solution obtained was used to restore digital images affected by noise. From this work, we can see that our model provides better image denoising than the Perona-Malik model and that of Catte et Al. More specifically, the proposed model with a colored noise effect provides better image denoising than the proposed model with a white noise effect.

References:-

- [1] Deriche R. and Faugeras O., Les equations aux derivees partielles en traitement des images et vision par ordinateur, *Revue Traitement du signal*, vol. 13, no. 6, pp. 551-577, 1996.
- [2] Bratsolis, E. and Sigelle, M. (2003), Fast SAR image restoration, segmentation, and detection of high- reflectance regions, *IEEE Trans. Geosci. Remote Sens*, Vol. 41, pp.2890–2899.
- [3] J. FOURIER, 1822, *Theorie analytique de la chaleur*.
- [4] J.MALIK and P.PERONA, Scale-Space and Edge Detection Using Anisotropic Diffusion, *IEEE Transactions on Pattern Analysis and Machine Intelligence*, 1987.
- [5] F.Catte, T.Coll, P.L.Lions and J.M.Morel, Image selective smoothing and edge detection by non linear diffusion(i), *SIAM J, Numer Anual*, 29(1) :182-193, February 1992.
- [6] M.Nitzberg and T.Shoita, Non linear image filtering with edge and corner enhancement, *IEEE transactions on Pattern Analysis and Machine intelligence*, 14(8) :826- 832, 1992.
- [7] LACHACHE Mohamed, Etude d'existence et d'unicite de la solution du modèle de Catte et al., *Memoire de Master de Mathematiques et Informatique*, Universite Mohamed Boudiaf de M'sila, Juin 2019.
- [8] S. Morfu, On some applications of diffusion processes for image processing, *Physics Letters A* 373 (2009), 2438-2444.
- [9] V. M. Serge Soumanou¹, Sounmaila Moumouni, Siaka Massou and Adebayo L. Essoun, 2020 Application of the digital resolution of anisotropic and nonlinear diffusion equation to image processing, *Advances in Differential Equations and Control Processes*, Volume 23, Number 2, Pages 105-123.
- [10] Adebayo L. ESSOUN, Etude stochastique de l'interaction des particules par une source unique aleatoire et Dynamique non lineaire avec fluctuation des paramètres cinetiques, thèse de doctorat, Universite d'Abomey-Calavi, 2014.
- [11] J. MOREL et T. COLL F. CATTE, P. LIONS, Image Selective Smoothing and Edge Detection by Nonlinear Diffusion, *Society for Industrial and Applied Mathematics*, Feb, 1992.
- [12] L.C.EVANS, partial differential equations, *proceedings of the American Mathematical society*, 1998.
- [13] H.BREZIS, ANALYSE FONCTIONNELLE Theorie et applications, *Universite Pierre et Marie Curie et ecole Polytechnique*, 1987.

- [14] A.Ralph, Topics in nonlinear functional analysis, UNIVERSITE BORDEAUX I, 2001.
- [15] R.ADAMS, Sobolev spaces, Academic Press, New York - San Francisco - London, 1975.
- [16] M. Black, G. Sapiro, D. Marimont, D. Heeger Robust anisotropic diffusion, IEEE Transactions on Image Processing, vol.7, no.3, pp. 421-432, March 1998, DOI : 10.1109/83.661192.
- [17] R. Whitaker, Geometry limited diffusion, Thèse de doctorat, Department of Computer Science, University of North Carolina, 1993.
- [18] Veronique SERFATY et Bruno MIGEON, filtrage EPSF «edge preserving smoothing filter» pour l'amélioration de l'image. INRIA Janvier 1994.